# Supplementary Information

## A generic high-dexterity soft neuroprosthetic hand for daily activities

Ningbin Zhang[1#], Xinyu Yang[1#], Zheng Zong[1], Yang Yu[2], Yi Zhao[1], Rong Bian[1], Chenru Jiang[1], Fengjie Shen[1], Xiangyang Zhu[1,2*], Guoying Gu[1,2*]

[1]Robotics Institute, State Key Laboratory of Mechanical System and Vibration, School of Mechanical Engineering, Shanghai Jiao Tong University, Shanghai 200240, China.
[2]Shanghai Key Laboratory of Intelligent Robotics, Shanghai Jiao Tong University, Shanghai 200240, China.

[#]These authors contributed equally to this work.
[*]Corresponding author. Email: guguoying@sjtu.edu.cn, mexyzhu@sjtu.edu.cn.

**The PDF file includes:**



**Other Supplementary Information for this manuscript includes the following:**

# Supplementary Text 1

## Analytical modelling of finger segments

We develop an analytical model of the fiber-reinforced soft finger segment (**Extended Data Fig. 1b**). In the finger segment, the elastomeric chamber is approximated as a rectangular prism. Its thickness, inner height, and inner width are defined as $t$, $h$, and $w$, respectively. The elastomeric chamber is modelled as an incompressible Neo-Hookean material with an initial shear modulus of $\mu$. The polyethylene sheet is modeled as a flexible but inextensible layer. Initially, the soft finger segment exhibits an axial length of $L$. Under applied pneumatic pressure $P$, the axial elongation of the finger segment ($y$-direction) can be expressed as:

$$\lambda_z(y) = \frac{y\left(\lambda_z(h)-1\right)}{h}+1, \tag{S1}$$

where $\lambda_z(h) = \lambda_z^h = l/L$ denotes the axial stretch of the upper surface, and $l$ denotes the stretched length. The strain energy density of the elastomeric chamber, $W$, is given by

$$W = \frac{\mu\left(I_1-3\right)}{2}. \tag{S2}$$

The parameter $I_1$ is the first invariant of the deformation gradient $\mathbf{F}$:

$$I_1 = \mathrm{tr}\left(\mathbf{F}\mathbf{F}^{\mathrm{T}}\right) = \lambda_1^2+\lambda_2^2+\lambda_3^2. \tag{S3}$$

In equation S3, the deformation gradient $\mathbf{F}$ is expressed as:

$$\mathbf{F} = \begin{bmatrix} \lambda_1 & 0 & 0 \\ 0 & \lambda_2 & 0 \\ 0 & 0 & \lambda_3 \end{bmatrix} \tag{S4}$$

where $\lambda_1$, $\lambda_2$, and $\lambda_3$ denote the radial, circumferential, and axial stretches, respectively. Material incompressibility imposes the constraint:

$$\lambda_1 \cdot \lambda_2 \cdot \lambda_3 = 1. \tag{S5}$$

The circumferential constraint from fibers suppresses elastomeric chamber's torsional deformation, allowing the circumferential strain to be neglected ($\lambda_2 = 1$). Thus, we have:

$$\lambda_1 = \lambda_z^{-1}(y),\ \lambda_2 = 1,\ \lambda_3 = \lambda_z(y). \tag{S6}$$

The deformation gradient $\mathbf{F}$ can be rewritten as:

$$\mathbf{F} = \begin{bmatrix} \lambda_z^{-1}(y) & 0 & 0 \\ 0 & 1 & 0 \\ 0 & 0 & \lambda_z(y) \end{bmatrix}. \tag{S7}$$

By combining equations S2, S3 and S7, we obtain:

$$W=\frac{\mu\left(\left(\lambda_z^{-1}(y)\right)^2+\left(\lambda_z(y)\right)^2+1-3\right)}{2}. \tag{S8}$$

The principal nominal stresses $S_i$ ($i$ = 1,2,3) of the elastomeric chamber can be calculated by

$$S_i=\frac{\partial W}{\partial \lambda_i}-\frac{\xi}{\lambda_i}, \tag{S9}$$

where $\xi$ is the Lagrange multiplier. As the radial stress is negligible, we have:

$$S_1=\frac{\partial W}{\partial \lambda_1}-\frac{\xi}{\lambda_1}=\mu\lambda_1-\frac{\xi}{\lambda_1}=0. \tag{S10}$$

Thus, the Lagrange multiplier $\xi$ can be expressed as a function of $y$, which is solved by

$$\xi(y)=\mu\lambda_1^2=\mu\lambda_z^{-2}(y). \tag{S11}$$

By combining equations S9 and S11, the circumferential stress is derived:

$$S_2(y)=\frac{\partial W}{\partial \lambda_2}-\frac{\xi(y)}{\lambda_2}=\mu\left(1-\lambda_z^{-2}(y)\right)=\mu-\mu\left[\frac{y}{h}\left(\lambda_z^h-1\right)+1\right]^{-2}. \tag{S12}$$

The axial stress $S_3$ is calculated by

$$S_3(y)=\frac{\partial W}{\partial \lambda_3}-\frac{\xi(y)}{\lambda_3}=\mu\left(\lambda_z(y)-\lambda_z^{-3}(y)\right)=\mu\left[\frac{y}{h}\left(\lambda_z^h-1\right)+1\right]-\mu\left[\frac{y}{h}\left(\lambda_z^h-1\right)+1\right]^{-3}. \tag{S13}$$

The relationship between elastomeric chamber's bending angle $\alpha$ and parameters ($l$, $L$, and $h$) is established by

$$\alpha=\frac{l-L}{h}. \tag{S14}$$

The elastomeric chamber's bending motion arises from the moment $M_P$ induced by applied pressure $P$ acting on the end cap. The relationship between $P$ and $\alpha$ is derived by equating the moment $M_C$ (calculated from internal stresses) to $M_P$:

$$M_C=M_P. \tag{S15}$$

The neutral axis of bending is along the polyethylene sheet layer, thus $M_C$ is derived by

$$M_C=2\int_0^h S_3(y)ytdy+S_3(h)wht. \tag{S16}$$

The moment $M_P$ is expressed as

$$M_P=\int_0^h Pwydy. \tag{S17}$$

Solving equations S14-S17 yields the $P$-$\alpha$ relationship (with $\lambda_z^h$ as an intermediate variable):

$$\begin{cases}\dfrac{2t}{3w\left(\lambda_z^h-1\right)^2}\left[2\left(\lambda_z^h\right)^3-3\left(\lambda_z^h\right)^2+6\left(\lambda_z^h\right)^{-1}-3\left(\lambda_z^h\right)^{-2}-2\right]+\dfrac{2t}{h}\left[\left(\lambda_z^h\right)-\left(\lambda_z^h\right)^{-3}\right]=\dfrac{P}{\mu}\\ \alpha=\dfrac{(\lambda_z^h-1)L}{h}\end{cases}. \tag{S18}$$

# Supplementary Text 2

## Typical FSM-based control

Two sEMG channels (each with 2 states) generate $2^2 = 4$ combined states (i.e., “Execute current grasp mode”, “Release from current grasp mode”, “Switch to next grasp mode”, and “Rest”). This control strategy in principle allows cycling through all grasping modes that the hand mechanism can physically achieve, and the practical number of modes is tailored to the user’s preference, balancing functionality with the need to avoid an overly cumbersome cycling sequence. For any given grasp mode, the states of “Rest” and “Switch to next grasp mode” are reserved for global management, leaving only the “Execute current grasp mode” and “Release from current grasp mode” to control the grasp mode itself. This results in binary on/off grasps without further programmable modulation.

# Supplementary Text 3

**Measurement and calculation of postural compensation angles**

We use inertial measurement units (IMUs) to measure the amputee subject's postural compensations when he uses different neuroprosthetic hands in the light bulb manipulation task. To this end, three IMUs (Awinda, Xsens) are used to measure the joint angles of the elbow, shoulder, and waist (**Supplementary Fig. 10a-b**). Before measurements, all three IMUs are put in alignment with their z-axis parallelly pointing straight up and then uniformly calibrated (**Supplementary Fig. 10c-d**), by which their coordinate frames are unified using data collection software (MT Manager 2022, Xsens). IMU-1 is attached to the amputee subject's chest with its x-axis in alignment with the central axis of the main body. IMU-2 and IMU-3 are respectively attached to the upper arm and forearm, with their x-axis in alignment with them (**Supplementary Fig. 10e**). During the experiment, the data collection software records the pose of all the IMUs in the entire process in the form of Euler angles. From the recorded data, we obtain the coordination system information of all IMUs, by which the joint angle can be calculated. The x-axis of IMU-1 is used to generate the waist abduction and flexion angle by projection to calibrated coordinate planes. The information from IMU-1 and IMU-2 is used to generate the shoulder abduction and flexion angle by projecting the x-axis of IMU-2 to the coordinate planes of IMU-1. The x-axis information of IMU-2 and IMU-3 is used to calculate the elbow flexion angle (**Supplementary Fig. 10f**). After the joint angle variations during the task are obtained, all the joints' compensation motion ranges are obtained by making a difference between the maximum and minimum joint angles (**Supplementary Fig. 10g**). The calculation procedures are as follows:

$$ {}^{n}_{m}\mathbf{R} = \begin{pmatrix} {}^{n}_{m}\mathbf{x} & {}^{n}_{m}\mathbf{y} & {}^{n}_{m}\mathbf{z} \end{pmatrix} = \begin{bmatrix} {}^{n}_{m}a & {}^{n}_{m}d & {}^{n}_{m}g \\ {}^{n}_{m}b & {}^{n}_{m}e & {}^{n}_{m}h \\ {}^{n}_{m}c & {}^{n}_{m}f & {}^{n}_{m}i \end{bmatrix} \tag{S19} $$

$$ \begin{aligned} \theta_{wa} &= \arctan\left(\frac{{}^{0}_{1}b}{{}^{0}_{1}c}\right), \theta_{wf} = \arctan\left(\frac{{}^{0}_{1}a}{{}^{0}_{1}c}\right), \theta_{sa} = \arctan\left(\frac{-{}^{1}_{2}b}{{}^{1}_{2}a}\right), \\ \theta_{sf} &= \arctan\left(\frac{-{}^{1}_{2}c}{{}^{1}_{2}a}\right), \theta_{ef} = 180° - \arctan\left(\frac{\overrightarrow{{}^{0}_{1}\boldsymbol{x}} \cdot \overrightarrow{{}^{0}_{2}\boldsymbol{x}}}{\left|\overrightarrow{{}^{0}_{1}\boldsymbol{x}}\right| \left|\overrightarrow{{}^{0}_{2}\boldsymbol{x}}\right|}\right) \end{aligned} \tag{S20} $$

Here, $\theta_{wa}$, $\theta_{wf}$, $\theta_{sa}$, $\theta_{sf}$, $\theta_{ef}$ stands for the joint angle of waist abduction, waist flexion, shoulder abduction, shoulder flexion and elbow flexion, respectively. ${}^{n}_{m}\mathbf{R} = \begin{pmatrix} {}^{n}_{m}\mathbf{x} & {}^{n}_{m}\mathbf{y} & {}^{n}_{m}\mathbf{z} \end{pmatrix}$ represents the *x, y, z* axes of the *m*th IMU's coordinate system expressed in the *n*th IMU's coordinate system, where ${}^{n}_{m}\mathbf{R}$ for all the IMUs can be obtained directly by measurement.

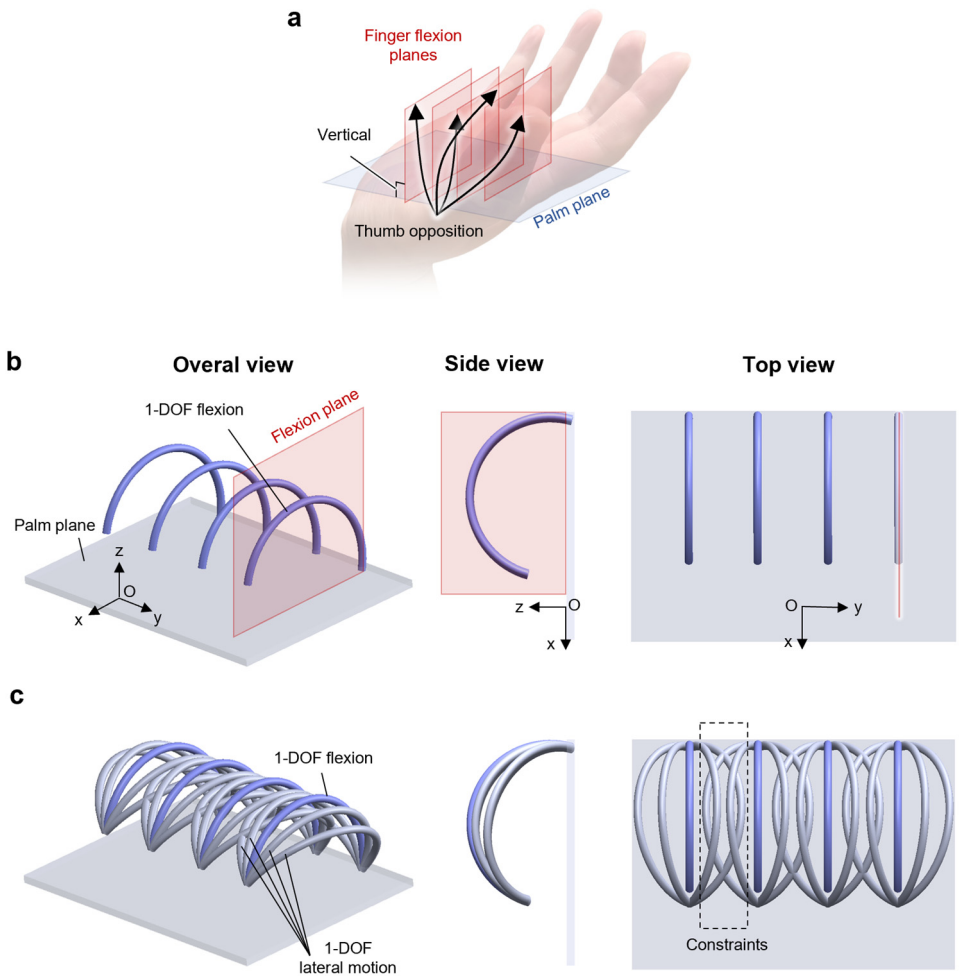


**Supplementary Fig. 1. Design prioritization among multiple DOFs. a**, Schematic principle of finger flexion in the human hand. The four fingers flex in approximately parallel planes (flexion planes) nearly vertical to the palm. These motions coordinate with thumb movement, and their combined kinematics give rise to the primary function of thumb opposition. **b**, Schematic principle of a prosthetic hand with active 1-DOF finger flexion. The side view shows that motion in the flexion plane follows a curved trajectory, which results in a limited workspace within this plane. **c**, Schematic principle of active 2-DOF finger flexion and lateral motion. The side view and top view show that the workspace within the flexion plane remains limited, a constraint that is further compounded by physical interference from adjacent fingers. Yet, under external forces or actions from adjacent fingers and the opposable thumb, this very interference can induce soft fingers' passive lateral motion for adaptive grasp and manipulation. Therefore, finger lateral motion is not eliminated but achieved through a form of embodied intelligence.

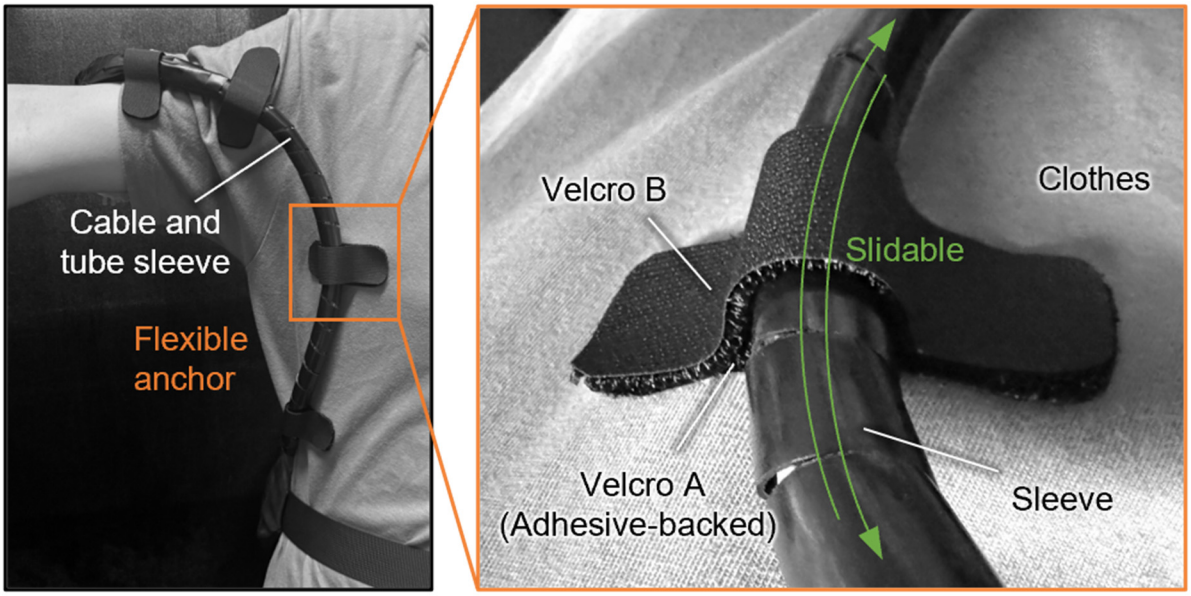


**Supplementary Fig. 2. Flexible Velcro-based anchors for cable and tube routing.** These anchors are designed to be attached to the user's clothing, conforming to body movements for adaptable routing. Each anchor consists of two Vlecro parts (A and B). Part A features an adhesive backing for secure attachment to fabrics and is shaped to preserve an "Ω"-shaped space. Part B physically attaches to Part A through a hook-and-loop interface, thereby enabling a secure connection that is also easily adjustable and detachable. The sleeve containing the electrical wires and pneumatic tubes is slidable within this "Ω"-shaped Velcro pair, thus minimizing interference during body movement and social interactions. Additionally, the bag is constructed from a lightweight nylon material to maintain a low profile, even when worn over thicker clothing.

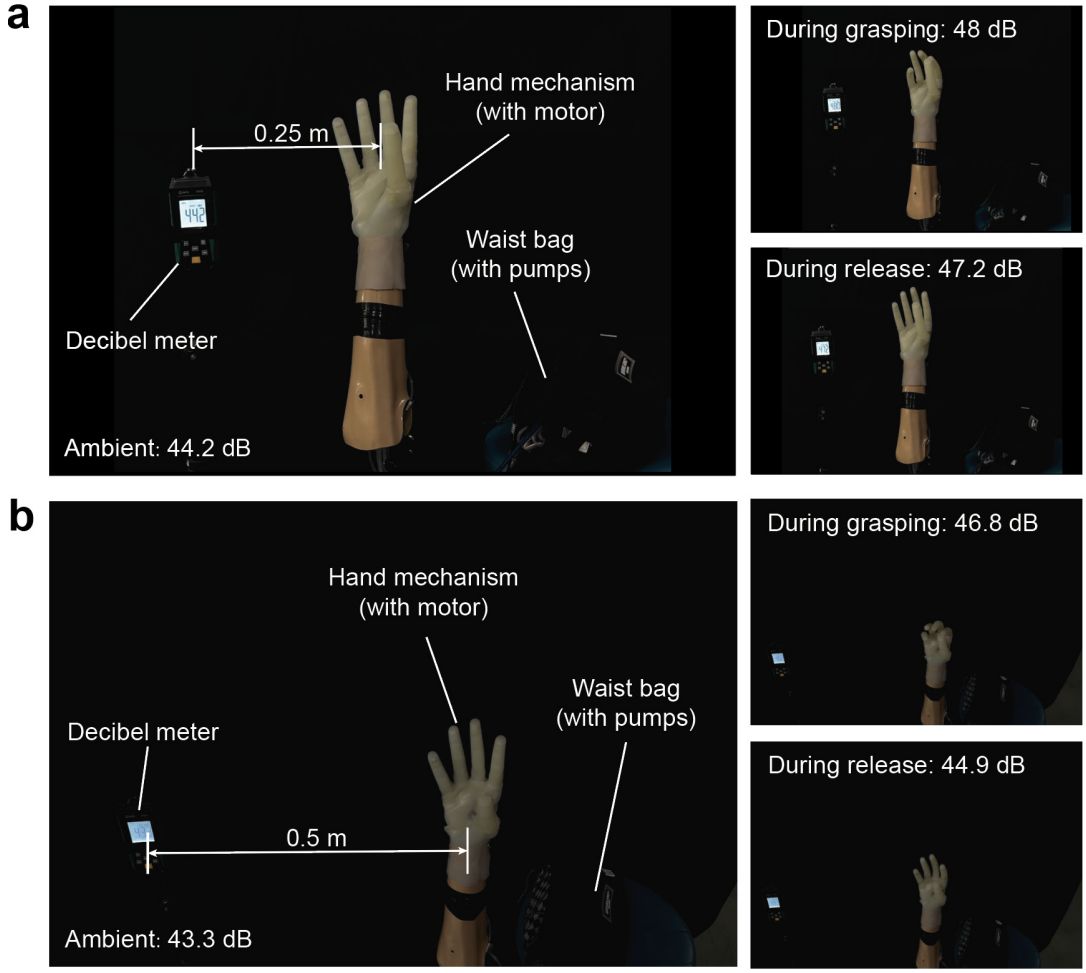


**Supplementary Fig. 3. Noise measurements. a**, Setup for measurement at a distance of 0.25 m using a decibel meter. With the motor in the hand and pumps in the waist bag, the recorded levels are 44.2 dB (ambient), 48.0 dB (during grasp), and 47.2 dB (during release). **b**, Setup for measurement at a distance of 0.5 m using the same decibel meter. The recorded levels are 43.3 dB (ambient), 46.8 dB (during grasping), and 44.9 dB (during release).

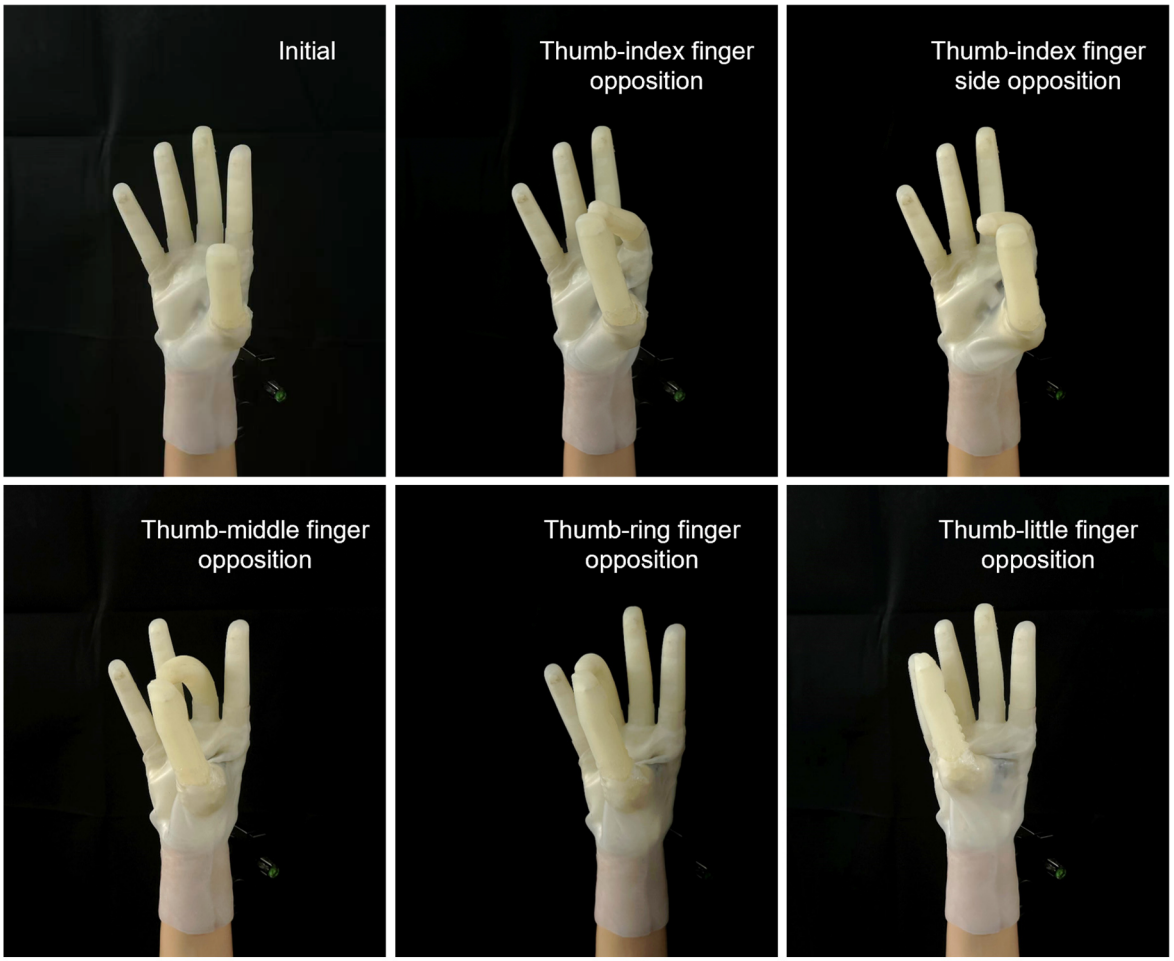


**Supplementary Fig. 4. Demonstration of thumb opposition with other fingers.** The opposition is achieved by the coordinated motion of the thumb-palm composite and fingers.

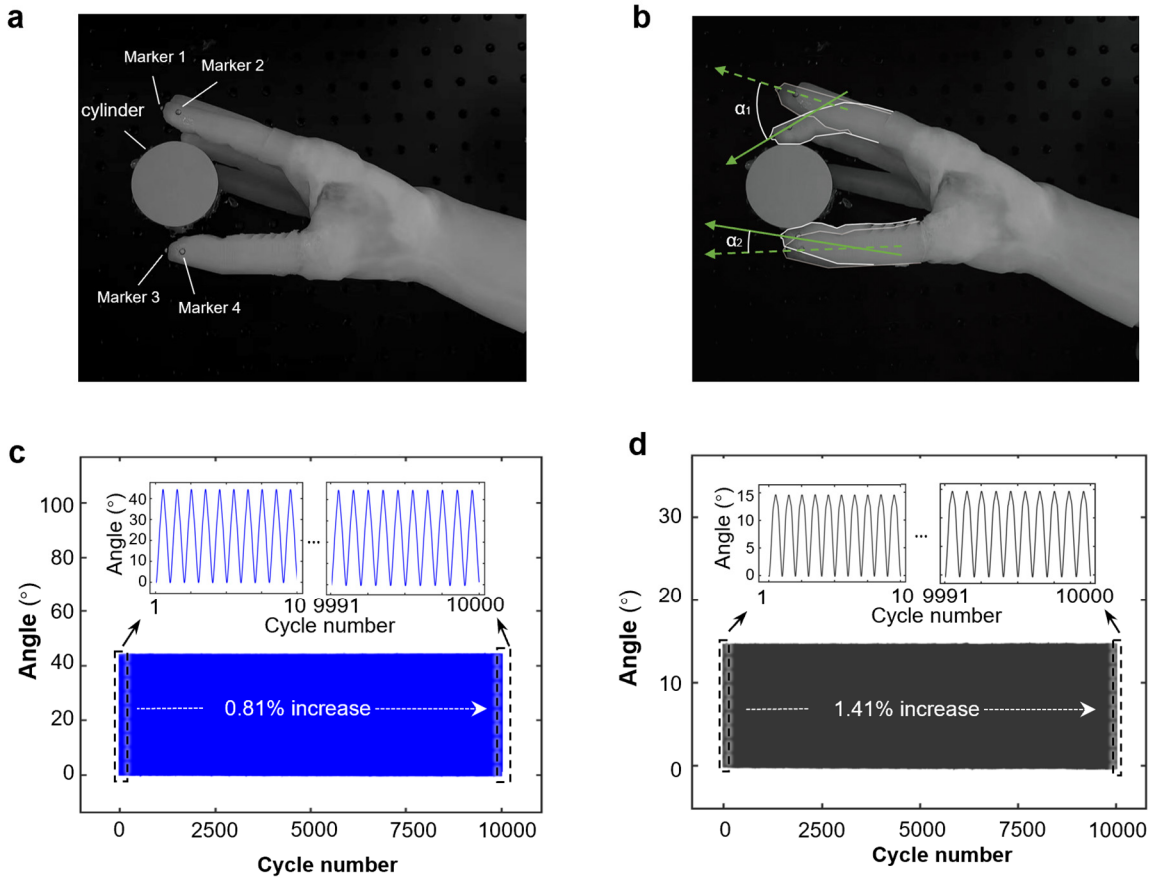


**Supplementary Fig. 5. Durability test with object contact.** **a**, Description of the experimental setup. We mount DexSoftNeuroHand and a cylinder (diameter: 60 mm) on the test table. Markers 1 and 2 are attached to the index finger, while markers 3 and 4 are placed on the thumb. A pneumatic system applies periodic actuation pressure (0-100 kPa) at 2-second intervals to control DexSoftNeuroHand to grasp and release, with the actuation cycle repeated over 10,000 cycles. **b**, Schematic illustration of the grasping process with flexion angle annotations. The flexion angle of the index finger ($\alpha_1$) and that of the thumb ($\alpha_2$) are calculated based on the vectors formed by the paired markers. **c**, Variation in the finger flexion angle during 10,000 grasping cycles. The flexion angle of the index finger remains stable throughout the durability test, with no significant changes observed (only 0.81% increase). **d**, Variation in the thumb flexion angle during 10,000 grasping cycles. Similar to the index finger, the thumb maintains a stable flexion angle throughout the test (only 1.41% increase), confirming the long-term reliability.

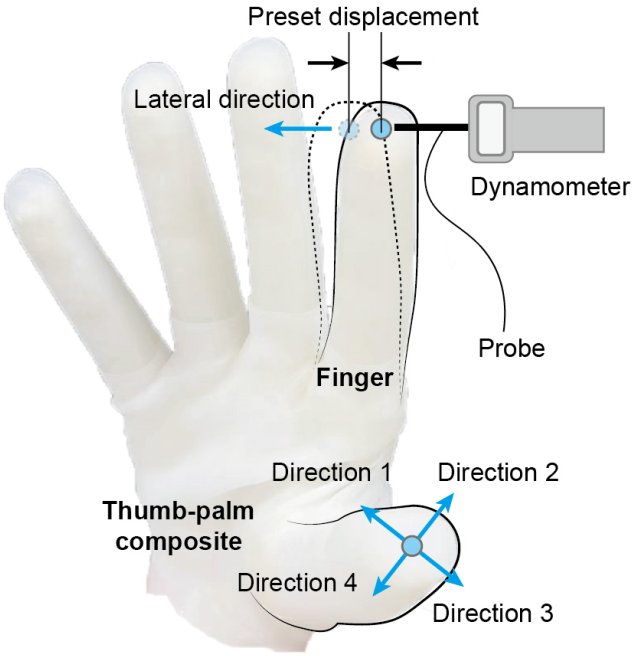


**Supplementary Fig. 6. Stiffness measurement setup for the finger and thumb-palm composite.** Finger (lateral) and thumb-palm composite (four directions) stiffnesses are evaluated by applying a preset displacement ($\Delta d$ = 10 mm) and measuring the force ($f$) from a dynamometer with a probe. Stiffness is given by $k = f / \Delta d$.

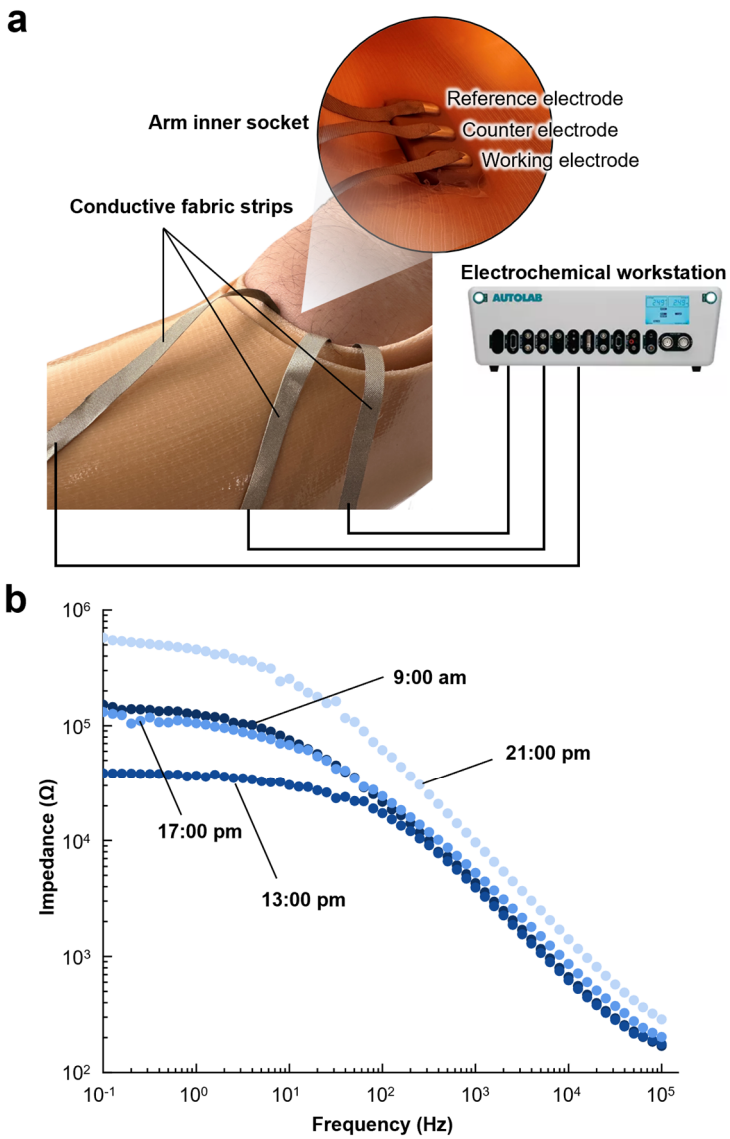


**Supplementary Fig. 7. Skin impedance evaluations with the sEMG sensor. a**, Experimental setups on the amputee subject 1. **b**, Skin impedances as functions of the frequency. The impedance measurements are performed at 4-hour intervals within 12 hours.

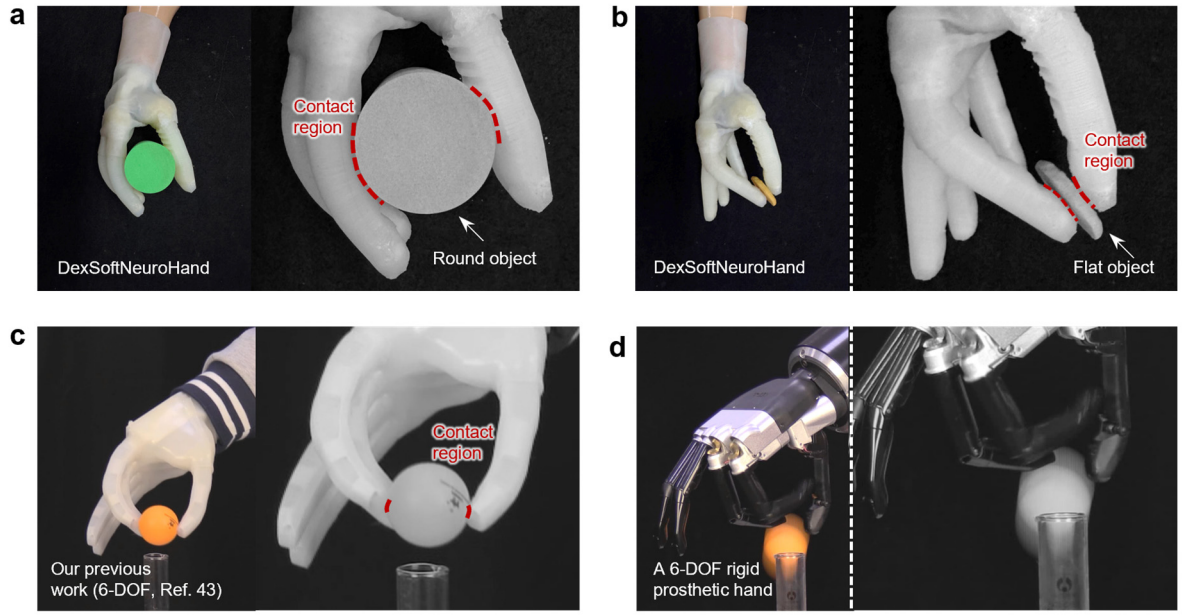


**Supplementary Fig. 8. Grasping advantages. a-b**, DexSoftNeuroHand enables adaptive contact with sufficient regions during grasping through high-DOF coordination, as seen in tasks like power grasping a round object or pinching a flat one. **c**, The 6-DOF soft neuroprosthetic hand from our previous work, typically with only one active flexion DOF per finger, performs pinches with limited contact areas that can lead to instability[42]. **d**, During pinching, a 6-DOF rigid prosthetic hand exhibits limited contact areas and a lack of compliance.

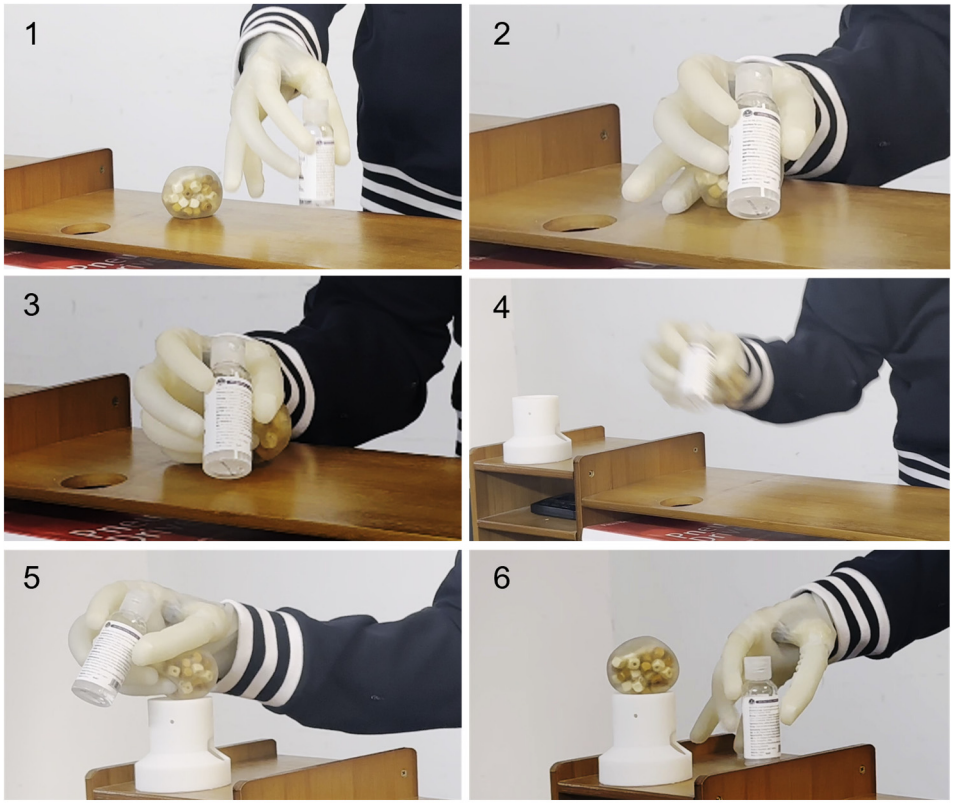


**Supplementary Fig. 9. Pick and place of two objects.** DexSoftNeuroHand enables the amputee to pick and retain one object within the hand while picking a second one, followed by sequentially placing both, unlike the conventional prostheses that need releasing an object before picking up a new one (see Supplementary Video 14 for details).

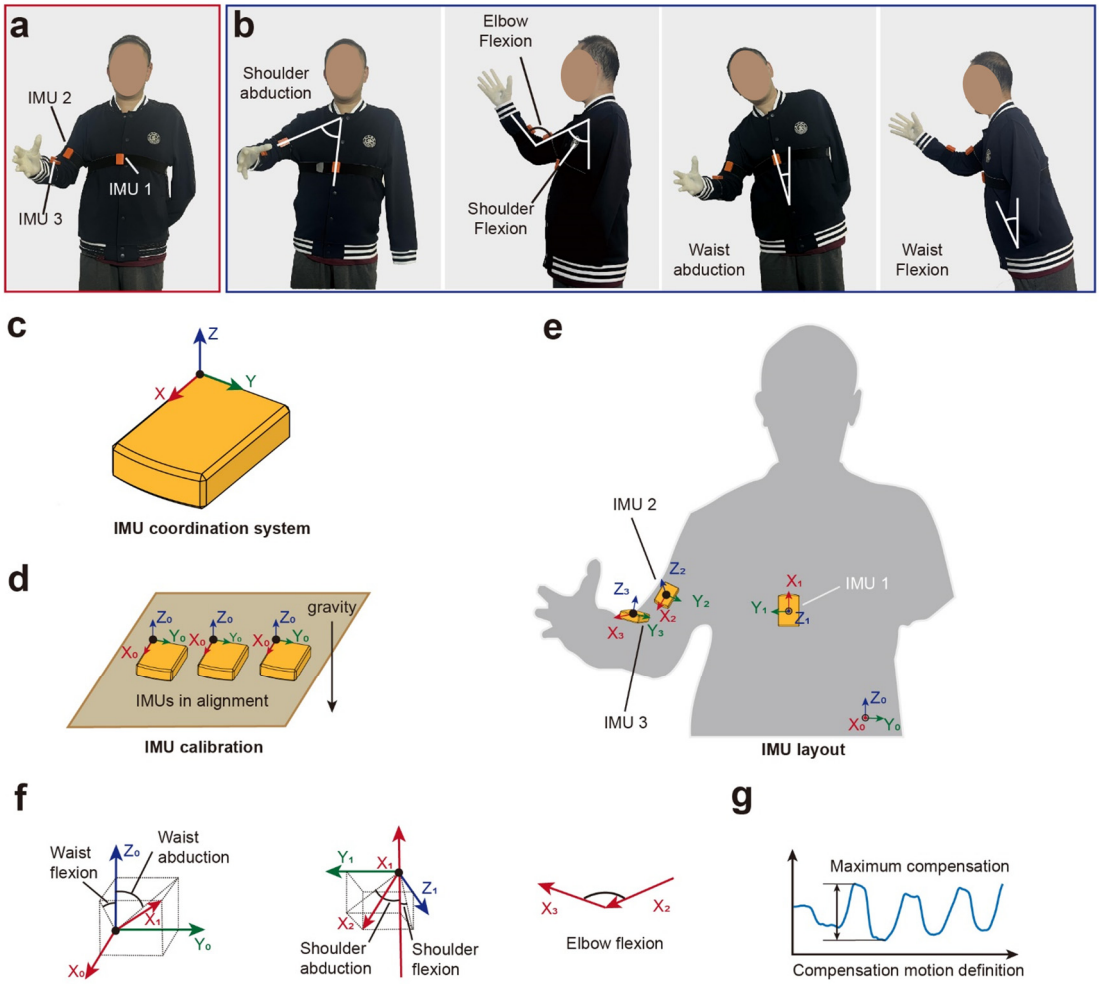


**Supplementary Fig. 10. Measurement and calculation of the body postural compensation angles.** **a**, The IMU sensor arrangement on the subject to measure the body postural compensation angle. **b**, The definition of the main body compensation angles. **c**, The coordination system of the IMU sensor. **d**, The calibration process of the IMU sensors before the experiment. All the IMU sensors are put in alignment and calibrated to share the same coordinate system layout with the $Z_0$ axis opposite the gravity direction. **e**, The IMU layout on the amputee subject and the corresponding coordinate systems. The IMU 1 is put on the chest of the subject to measure the waist compensation angles with its $X_1$ axis parallel to the main body's central axis. The IMU 2 and IMU 3 are put on the upper limb and forearm, respectively, with their $X$-axes parallel to the corresponding limbs to measure the compensation angles of the shoulder and elbow. **f**, The calculation method of the five body compensation angles. **g**, The maximum compensation angle is defined as the difference between the maximum and minimum joint angle of the joint angle curve during the manipulation task.

## Supplementary Table 1

Comparison of DexSoftNeuroHand with existing prosthetic hands in key design characteristics. SMA, Shape-memory alloy; sEMG, surface electromyography; FSM, finite state machine; PR, pattern recognition; NP, not provided; *, the glove weight is not included; #, these systems are developed as commercial products; consequently, their sEMG sensor configurations and algorithms are proprietary and subject to change across firmware updates.

| | Actuation method | Active DOFs | Self-adapting mechanisms | Control method | Weight (g) |
|---|---|---|---|---|---|
| Michelangelo (Ref. 2) | Motor +linkage | 2 | Linkages with local compliant elements | sEMG# | 510* |
| Vincent (Ref. 15) | Motor +linkage | 6 | Linkages with local compliant elements | sEMG# | 485* |
| i-Limb (Ref. 2) | Motor +linkage | 6 | Linkages with local compliant elements | sEMG# | 628* |
| Bebionic (Ref. 15) | Motor +linkage | 5 | Linkages with local compliant elements | sEMG# | 588* |
| Hannes (Ref. 16) | Motor +tendon | 1 | Rigid skeletons with synergistic elements | sEMG | 480* |
| Pisa/IIT hand (Ref. 18) | Motor +tendon | 1 | Dislocatable joint +rigid skeletons | NP | NP |
| Pisa/IIT hand 2 (Ref. 19) | Motor +tendon | 2 | Dislocatable joint +rigid skeletons | sEMG | ~500* |
| X-Limb (Ref. 38) | Motor +tendon | 5 | flexure joint +semi-rigid skeletons | NP | 253 |
| X hand (Ref. 14) | Motor +tendon | 2 | NP | NP | NP |
| DEKA (Ref. 13) | Motor +linkage | 4 | NP | sEMG | 1400 |
| Smart hand (Ref. 11) | Motor +tendon | 4 | NP | sEMG | 530* |
| SSSA-Myhand (Ref. 12) | Motor +linkage | 3 | NP | sEMG | 478* |
| SoftHand Pro-2 (Ref. 23) | Motor +tendon | 2 | Dislocatable joint +rigid skeletons | sEMG | NP |
| HANDSON (Ref. 32) | Motor +linkage | 3 | Linkages with local compliant elements | sEMG | NP |
| 19-DOF hand (Ref. 33) | SMA +tendon | 19 | NP | Voice | 220* |
| Hybrid hand (Ref. 46) | Pneumatic | 14 | Soft joints +rigid skeletons | sEMG | NP |
| Our prior work (Ref. 43) | Pneumatic | 6 | Soft continuous body+rigid skeletons | sEMG | Hand mechanism: 292 Total: 736 |
| **This work** | **Pneumatic +motor** | **11** | **Soft continuous body +rigid revolute joint and skeletons** | **sEMG** | **Hand mechanism: 242 Total: 703** |

## Supplementary Table 2

Comparison of DexSoftNeuroHand with existing prosthetic hands in mechanical performances. NP, not provided; F-E, flexion-extension; A-A, abduction-adduction.

| | Active finger kinematics | Compliance directions | Finger force (N) | Hand payload (N) | Finger speed (°/s) |
|---|---|---|---|---|---|
| Michelangelo (Ref. 2) | Coupled all fingers' motion | F-E | NP | 78.14 | 86.9 |
| Vincent (Ref. 15) | Coupled MCP/PIP flexion | F-E | 3~8.44 | NP | 87.9~103.3 |
| i-Limb (Ref. 2) | Coupled MCP/PIP flexion | F-E | 3.09~11.18 | 71.44 | 60.5~110.6 |
| Bebionic (Ref. 15) | Coupled MCP/PIP flexion | F-E | 12.25~16.11 | 77.37 | 36.6~96.4 |
| Hannes (Ref. 16) | Coupled multi-joint motions | F-E, A-A | NP | 51~141 | 150 |
| Pisa/IIT hand (Ref. 18) | Coupled multi-joint motion | Omni-directional | NP | 28 | NP |
| Pisa/IIT hand 2 (Ref. 19) | Coupled multi-joint motion | Omni-directional | NP | NP | NP |
| X-Limb (Ref. 38) | Coupled multi-joint flexion | Mainly F-E | NP | 21.5 | NP |
| X hand (Ref. 14) | Coupled four fingers' motion | Differential mechanism | NP | 8.82 | NP |
| DEKA hand (Ref. 13) | NP | NP | NP | NP | NP |
| Smart hand (Ref. 11) | Coupled multi-joint motion | Mainly F-E | NP | 98 | NP |
| SSSA-Myhand (Ref. 12) | Coupled multi-joint motion | NP | 11.7~31.4 | NP | 160~170 |
| SoftHand Pro-2 (Ref. 23) | Decoupled thumb abduction + coupled all finger flexion | F-E | NP | NP | NP |
| HANDSON (Ref. 32) | Two-finger gripper with coupled flexion | NP | NP | NP | NP |
| 19-DOF hand (Ref. 33) | Decoupled MCP and PIP flexion + MCP abduction | Omni-directional | NP | 24.5 | 63 |
| Hybrid hand (Ref. 46) | Decoupled MCP, PIP and DIP flexion | NP | 1.8 | >16 | NP |
| Our prior work (Ref. 43) | Coupled MCP, PIP and DIP flexion | Omni-directional | 1.9 | >20 | 105 |
| **This work** | **Decoupled MCP and (PIP+DIP) flexion** | **Omni-directional** | **Thumb: 3.5 Finger: 2.6** | **>25** | **110** |

## Supplementary Table 3

Comparison of DexSoftNeuroHand with existing prosthetic hands in key functionalities and amputee validations. NP, not provided.

| | Grasping | Manipulation | Amputee validation |
|---|---|---|---|
| Michelangelo (Ref. 2) | Lateral, palmar | No | Post-commercially validated |
| Vincent (Ref. 15) | NP | No | Post-commercially validated |
| i-Limb (Ref. 2) | Lateral, palmar, power | No | Post-commercially validated |
| Bebionic hand (Ref. 15) | Lateral, palmar, power | No | Post-commercially validated |
| Hannes (Ref. 16) | Lateral, precision, power | No | 3 male amputees, 29~62 years old |
| Pisa/IIT hand (Ref. 18) | Synergistic grasps | No | Able-bodied individuals fitted with a bypass prosthesis |
| Pisa/IIT hand 2 (Ref. 19) | Synergistic grasps | Non-amputee demonstration: object rotation, jar opening, coffee pouring | Able-bodied individuals fitted with a bypass prosthesis |
| X-Limb (Ref. 38) | Adaptive grasps: pinch, tripod, power | No | Able-bodied individuals fitted with a bypass prosthesis |
| X hand (Ref. 14) | 29 human-like postures | Non-amputee demonstration: ball/tweezer manipulation, cap screwing | No |
| DEKA hand (Ref. 13) | Pinch, tripod, power, lateral, precision | No | 21 amputees, 26~65 years old |
| Smart hand (Ref. 11) | Pinch, power, lateral, precision, tool, chuck | No | NP |
| SSSA-Myhand (Ref. 12) | Power, lateral, precision | No | NP |
| SoftHand Pro-2 (Ref. 23) | Power, pinch, tripod | Simple in-hand manipulation with tethered devices | 3 female amputees, 37.3±3.5 years old |
| HANDSON (Ref. 32) | power, pinch, precision | Bulb installation | 1 female amputee, 50 years old |
| 19-DOF hand (Ref. 33) | 33 human-like postures | Non-amputee demonstration: syringe and scissor use | 1 female amputee |
| Hybrid hand (Ref. 46) | Spherical, pinch, power, tripod, cylindrical (demonstration with tethered devices) | No | Robotic arm or able-bodied individuals fitted with a bypass prosthesis |
| Our prior work (Ref. 43) | Power, pinch, lateral, precision disk | No | 2 male amputees |
| **This work** | **32 human-like adaptive postures, safe and compliant interaction** | **Continuous scissors use, pick and place two objects, Bulb installation** | **4 amputees, 38~70 years old, 3 males, 1 female** |

## Supplementary Table 4

Detailed information of DexSoftNeuroHand's main components.

| Component | Dimension (mm×mm×mm) | Weight (g) | Materials and parameters of the component | Price (USD) |
|---|---|---|---|---|
| **Hand mechanism (total weight of 242 g)** | | | | |
| Thumb | 100×24×20 | 20 | Elastomeric chamber: Dragonskin 20; Skin: Ecoflex 0030; | 3 |
| Index, middle, ring, and little fingers | 110×24×20 (per piece) | 78 (4 pieces) | | 12 |
| Thumb-palm connection linkage | 75×50×20 | 36.5 | 3D printed with resin (8200, Wenext) | 3 |
| Palm with skin | 94×78×132 | 100 | Palm skeleton: 3D printed with resin (8200, Wenext); Skin: fabricated from Ecoflex 0035 | 22 |
| Servomotor | 23×9×16.7 | 7.5 | Speed: 0.09s; Torque: 3.3 kg-cm | 81.25 |
| **Pneumatic control systems in a waist bag (total weight of 461 g)** | | | | |
| sEMG recognition and collection unit | 45×18×7.2 | 10 (2 pieces) | Arduino (nano) 5-12 V, 12-channel input/output pins | 22 |
| Pneumatic control unit | 78×50×7.8 | 15 | Arduino (mega) | 20 |
| Data storage unit | 24×30×1 | 2 | Voltage: 5 V | 1 |
| Timing module | 38×22×14 | 8 | Zave (DS3231) Voltage: 3.3-5.5V | 0.9 |
| PCB circuit board | 80×50×1.1 | 17 | Customized | 25 |
| Pump | 67×27×27 | 302 (10 pieces) | Maximum pressure: 185 kPa; Flow rate: 3.5 LPM; Voltage: 6 V | 50 |
| Valve | 23×12×8 | 38 (10 pieces) | Parker (X-valve), 2-way normal closed, directional, 12 V | 350 |
| Voltage regulator | 18×10×2.6 | 2 | Input voltage range: 4-36 V | ~6 |
| Battery | 57×29×22 | 67 | Voltage: 11.1 V | ~10 |
| **Customized arm socket** | | | | |
| Socket | 274×95×90 | 75~105 | Customized | ~30 |
| sEMG sensors | 35×22×10 | 10 (2 pieces) | Danyang Inc. | ~100 |
| Passive wrist | 45×45×19 | 25 | Customized | ~9 |

## Supplementary Table 5

Stiffness characteristics of hand components. Soft fingers with different chamber materials under 200-kPa actuation pressure show varied stiffnesses. The material Dragonskin 20 is selected as it provides higher finger stiffness for improved operational stability while achieving sufficient bending angles within portable actuation constraints.

| **Material of the finger inner chamber** | **Measured finger stiffness** | **Finger bending angle** |
|---|---|---|
| Ecoflex 0030 | 8.2 ± 0.8 N/m | 356.4° |
| Dragonskin 10 | 33.4 ± 1.7 N/m | 197.8° |
| Dragonskin 20 | 61.0 ± 2.2 N/m | 183.2° |
| Dragonskin 30 | 89.3 ± 3.1 N/m | 75.6° |
| **Measured stiffness** | **Our previous work*** | **This work** |
| Finger | 24.6 ± 3.8 N/m | 61.0 ± 2.2 N/m |
| Thumb-palm composite (direction 1) | 15.0 ± 0.8 N/m | 169.0 ± 7.3 N/m |
| Thumb-palm composite (direction 2) | 12.7 ± 1.2 N/m | 168.3 ± 6.6 N/m |
| Thumb-palm composite (direction 3) | 16.7 ± 1.2 N/m | 168.0 ± 5.4 N/m |
| Thumb-palm composite (direction 4) | 15.3 ± 1.7 N/m | 163.5 ± 10.9 N/m |

*Gu, G. et al. A soft neuroprosthetic hand providing simultaneous myoelectric control and tactile feedback. *Nat. Biomed. Eng.* 7, 589-598 (2023).

## Supplementary Table 6

Control signal of grasp types. DOF 1, motor angle; DOF 2 to DOF 11, pump open time.

| | DOF 1 (°) | DOF 2 (ms) | DOF 3 (ms) | DOF 4 (ms) | DOF 5 (ms) | DOF 6 (ms) | DOF 7 (ms) | DOF 8 (ms) | DOF 9 (ms) | DOF 10 (ms) | DOF 11 (ms) |
|---|---|---|---|---|---|---|---|---|---|---|---|
| 1.Large diameter | 45 | 1000 | 1000 | 1000 | 1000 | 1000 | 1000 | 1000 | 1000 | 1000 | 1000 |
| 2.Small diameter | 45 | 1000 | 1000 | 1000 | 1000 | 1000 | 1000 | 1000 | 1000 | 1000 | 1000 |
| 3.Medium diameter | 45 | 1000 | 1000 | 1000 | 1000 | 1000 | 1000 | 1000 | 1000 | 1000 | 1000 |
| 4.Adducted thumb | 30 | 0 | 0 | 1000 | 1000 | 1000 | 1000 | 1000 | 1000 | 1000 | 1000 |
| 5.Light tool | 30 | 0 | 0 | 1000 | 1000 | 1000 | 1000 | 1000 | 1000 | 1000 | 1000 |
| 6.Prismatic 4 fingers | 45 | 500 | 500 | 500 | 250 | 500 | 250 | 500 | 250 | 500 | 250 |
| 7.Prismatic 3 fingers | 45 | 500 | 500 | 500 | 500 | 500 | 500 | 1000 | 1000 | 1000 | 1000 |
| 8.Prismatic 2 fingers | 45 | 500 | 500 | 500 | 500 | 1000 | 1000 | 1000 | 1000 | 1000 | 1000 |
| 9.Palmar pinch | 45 | 600 | 600 | 600 | 600 | 0 | 0 | 0 | 0 | 0 | 0 |
| 10.Power disk | 30 | 1000 | 1000 | 1000 | 1000 | 1000 | 1000 | 1000 | 1000 | 1000 | 1000 |
| 11.Power sphere | 30 | 1000 | 1000 | 1000 | 1000 | 1000 | 1000 | 1000 | 1000 | 1000 | 1000 |
| 12.Precision disk | 45 | 500 | 500 | 500 | 500 | 500 | 500 | 500 | 500 | 500 | 500 |
| 13.Precision sphere | 45 | 500 | 500 | 500 | 500 | 500 | 500 | 500 | 500 | 500 | 500 |
| 14.Tripod | 45 | 500 | 500 | 500 | 500 | 500 | 500 | 1000 | 1000 | 1000 | 1000 |
| 15.Fixed hook | 30 | 0 | 0 | 1000 | 1000 | 1000 | 1000 | 1000 | 1000 | 1000 | 1000 |
| 16.Lateral | 30 | 1000 | 1000 | 1000 | 1000 | 1000 | 1000 | 1000 | 1000 | 1000 | 1000 |
| 17.Index finger extension | 30 | 1000 | 0 | 0 | 0 | 1000 | 1000 | 1000 | 1000 | 1000 | 1000 |
| 18.Extension type | 30 | 1000 | 0 | 0 | 0 | 0 | 0 | 0 | 0 | 0 | 0 |
| 19.Distal type | 45 | 500 | 500 | 500 | 250 | 600 | 300 | 700 | 350 | 800 | 800 |
| 20.Writing tripod | 45 | 500 | 500 | 500 | 250 | 500 | 250 | 0 | 0 | 0 | 0 |
| 21.Tripod variation | 45 | 500 | 500 | 500 | 500 | 500 | 500 | 1000 | 1000 | 1000 | 1000 |
| 22.Parallel extension | 45 | 0 | 0 | 750 | 0 | 750 | 0 | 750 | 0 | 750 | 0 |
| 23.Adduction grip | 30 | 0 | 0 | 1000 | 1000 | 1000 | 1000 | 1000 | 1000 | 1000 | 1000 |
| 24.Tip pinch | 45 | 600 | 600 | 600 | 600 | 0 | 0 | 0 | 0 | 0 | 0 |
| 25.Lateral tripod | 45 | 500 | 500 | 500 | 500 | 500 | 500 | 1000 | 1000 | 1000 | 1000 |
| 26.Sphere 4 finger | 45 | 1000 | 1000 | 1000 | 1000 | 1000 | 1000 | 1000 | 1000 | 1000 | 1000 |
| 27.Quadpod | 45 | 500 | 500 | 500 | 500 | 500 | 500 | 500 | 500 | 0 | 0 |
| 28.Sphere 3 finger | 45 | 1000 | 1000 | 1000 | 1000 | 1000 | 1000 | 1000 | 1000 | 1000 | 1000 |
| 29.Stick | 45 | 600 | 600 | 1000 | 1000 | 1000 | 1000 | 1000 | 1000 | 1000 | 1000 |
| 30.Palmar Wrap | 30 | 1000 | 1000 | 1000 | 1000 | 1000 | 1000 | 1000 | 1000 | 1000 | 1000 |
| 31.Ring | 45 | 1000 | 1000 | 1000 | 1000 | 0 | 0 | 0 | 0 | 0 | 0 |
| 32.Ventral | 45 | 600 | 200 | 1000 | 1000 | 1000 | 1000 | 1000 | 1000 | 1000 | 1000 |
| 33.Inferior pincer | 45 | 600 | 600 | 600 | 600 | 0 | 0 | 0 | 0 | 0 | 0 |

## Supplementary Table 7

Basic information of the amputee subjects.

| Amputee | Age | Gender | Amputation | Prosthetic utilization | Frequent life scenarios |
|---|---|---|---|---|---|
| Subject 1 | 38 | Male | Right hand (below elbow disarticulation), Left hand (shoulder disarticulation) | Full-time | Independent living ability (e.g., dressing, feeding and cleaning tasks) |
| Subject 2 | 42 | Female | Right hand (wrist disarticulation) | Part-time | Household chores, intimate interaction in family caregiving roles, water-resistant functionality |
| Subject 3 | 46 | Male | Right hand (wrist disarticulation) | No | Operation in urban life (e.g., making coffee, driving and recreational activities) |
| Subject 4 | 70 | Male | Left hand (wrist disarticulation) | No | Life assistant (e.g., taking medicine) |

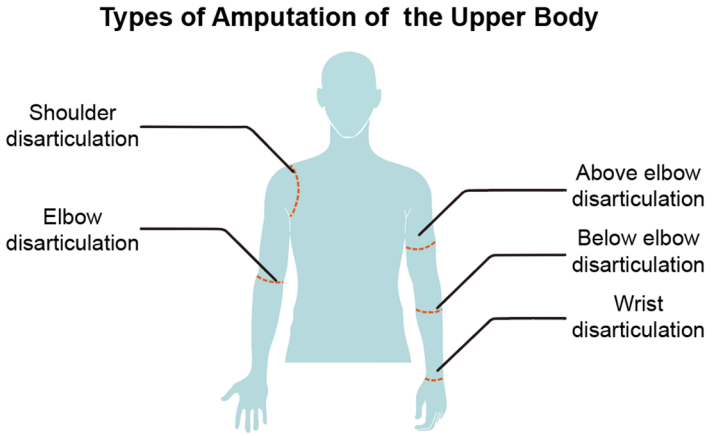

## Supplementary Table 8

The preset sEMG commands for 12-hour myoelectric tests, which are conducted at time sessions: 9:00, 13:00, 17:00, and 21:00. At each session, each amputee subject is instructed to perform a total of 50 preset sEMG commands in order, including 10 AC1s, 10 AC2s, 10 RLs, 10 SWs, and10 KEs.

| **Test time: 9:00** | | | | | | | | | | |
|---|---|---|---|---|---|---|---|---|---|---|
| **Command 1-10** | AC2 | AC1 | RL | SW | KE | AC2 | AC1 | RL | SW | KE |
| **Command 11-20** | AC2 | KE | AC2 | AC1 | SW | RL | AC1 | SW | RL | KE |
| **Command 21-30** | AC1 | AC2 | KE | AC2 | SW | AC1 | RL | KE | SW | RL |
| **Command 31-40** | RL | KE | RL | SW | AC1 | AC2 | AC1 | KE | SW | AC2 |
| **Command 41-50** | KE | AC1 | SW | AC2 | KE | RL | SW | AC2 | AC1 | RL |
| **Test time: 13:00** | | | | | | | | | | |
| **Command 1-10** | RL | KE | RL | AC2 | SW | AC1 | KE | SW | AC2 | AC1 |
| **Command 11-20** | AC1 | SW | AC2 | AC1 | KE | RL | AC2 | SW | KE | RL |
| **Command 21-30** | AC2 | RL | KE | AC1 | RL | SW | AC2 | KE | AC1 | SW |
| **Command 31-40** | SW | AC1 | RL | KE | SW | AC2 | AC1 | RL | KE | AC2 |
| **Command 41-50** | KE | AC2 | SW | AC1 | RL | KE | AC2 | SW | AC1 | RL |
| **Test time: 17:00** | | | | | | | | | | |
| **Command 1-10** | AC1 | KE | AC2 | AC1 | SW | RL | KE | AC2 | RL | SW |
| **Command 11-20** | SW | AC2 | RL | SW | KE | AC1 | AC2 | RL | KE | AC1 |
| **Command 21-30** | RL | KE | AC1 | RL | AC2 | SW | KE | AC1 | AC2 | SW |
| **Command 31-40** | AC2 | SW | KE | AC2 | AC1 | RL | SW | KE | AC1 | RL |
| **Command 41-50** | AC1 | RL | AC2 | KE | AC1 | SW | RL | AC2 | KE | SW |
| **Test time: 21:00** | | | | | | | | | | |
| **Command 1-10** | RL | KE | AC2 | SW | RL | AC1 | KE | AC2 | SW | AC1 |
| **Command 11-20** | SW | AC2 | AC1 | KE | SW | RL | AC2 | AC1 | KE | RL |
| **Command 21-30** | KE | AC1 | RL | AC2 | KE | SW | AC1 | RL | AC2 | SW |
| **Command 31-40** | AC2 | SW | KE | AC1 | AC2 | RL | SW | KE | AC1 | RL |
| **Command 41-50** | RL | AC1 | SW | KE | RL | AC2 | AC1 | SW | KE | AC2 |

## Supplementary Table 9

The sEMG signal thresholds for different amputee subjects.

| Amputee subject | AT1 (V) | RT1 (V) | AT2 (V) | Time threshold (ms) |
|---|---|---|---|---|
| Subject 1 | 0.98 | 0.38 | 1.28 | 300 |
| Subject 2 | 1.13 | 0.16 | 1.29 | 300 |
| Subject 3 | 0.97 | 0.10 | 0.81 | 200 |
| Subject 4 | 1.61 | 0.48 | 0.97 | 300 |

AT1, action threshold of the processed sEMG 1. RT1, rest threshold of the processed sEMG 1. AT2, action threshold of the processed sEMG 2.

## Supplementary Table 10

Detailed evaluation results of the Box and Blocks Test.

| Amputee subject | Block number | | | Average block number | Standard deviation |
|---|---|---|---|---|---|
| | 1st | 2nd | 3rd | | |
| Subject 1 | 27 | 29 | 30 | 28.67 | 1.25 |
| Subject 2 | 25 | 25 | 29 | 26.33 | 1.89 |
| Subject 3 | 23 | 23 | 22 | 22.67 | 0.47 |
| Subject 4 | 17 | 19 | 20 | 18.67 | 1.25 |

## Supplementary Table 11

A comparison of BBT scores among DexSoftNeuroHand, our previous work, and current neuroprosthetic hands.

| | **Ref. 1*** | **Ref. 2**** | **Ref. 3***** | **Our previous work******** | **This work** |
|---|---|---|---|---|---|
| Number of blocks | 14.3 | 26 | 24 | 16.3 | **18.7-28.7** |
| | *Resnik, L. et al. Reliability and validity of outcome measures for upper limb amputation. *J. Prosthet. Orthot.* 24, 192-201 (2012).<br>**Smit, G., et al. The lightweight Delft Cylinder Hand: first multi-articulating hand that meets the basic user requirements. *IEEE Trans. Neural Syst. Rehabil. Eng.* 23, 431-440 (2014).<br>***Phillips, S. L., et al. Experiences and outcomes with powered partial hand prostheses: a case series of subjects with multiple limb amputations. *J. Prosthet. Orthot.* 24, 93-97 (2012).<br>****Gu, G. et al. A soft neuroprosthetic hand providing simultaneous myoelectric control and tactile feedback. *Nat. Biomed. Eng.* 7, 589-598 (2023). | | | | |

## Supplementary Table 12

Detailed information of the objects used in the Southampton Hand Assessment Procedure.

| Task | Object name | Weight (g) | Dimension (mm×mm×mm) |
|---|---|---|---|
| S1 | Light cylinder cup | 90 | 90×70×70 |
| S2 | Heavy cylinder cup | 290 | 90×70×70 |
| S3 | Light sphere | 56.9 | 66.7×66.7×66.7 |
| S4 | Heavy sphere | 242 | 70×70×70 |
| S5 | Small acrylic sheet | 6.6 | 25×50×5 |
| S6 | Small metal sheet | 46.8 | 25×50×5 |
| S7 | Large acrylic sheet | 13 | 50×50×5 |
| S8 | Large metal sheet | 88.2 | 50×50×5 |
| S9 | Light triangular prism | 9.6 | 43×43×50 |
| S10 | Heavy triangular prism | 109.6 | 43×43×50 |
| S11 | Light cup | 30.3 | 65×65×65 |
| S12 | Heavy cup | 130.2 | 65×65×65 |

## Supplementary Table 13

Detailed evaluation results of the SHAP.

| Amputee | Task | Completion time (s) | | | Average completion time (s) | Standard deviation (s) |
|---|---|---|---|---|---|---|
| | | 1st | 2nd | 3rd | | |
| Subject 1 | S1 | 2.68 | 2.64 | 2.79 | 2.70 | 0.06 |
| | S2 | 2.72 | 2.56 | 2.42 | 2.57 | 0.12 |
| | S3 | 2.03 | 2.07 | 2.11 | 2.07 | 0.03 |
| | S4 | 2.85 | 2.81 | 2.50 | 2.72 | 0.16 |
| | S5 | 3.75 | 3.48 | 3.48 | 3.57 | 0.13 |
| | S6 | 3.20 | 3.38 | 3.46 | 3.35 | 0.11 |
| | S7 | 3.01 | 2.60 | 2.75 | 2.79 | 0.17 |
| | S8 | 3.10 | 3.13 | 2.96 | 3.06 | 0.07 |
| | S9 | 2.77 | 2.64 | 2.74 | 2.72 | 0.06 |
| | S10 | 3.04 | 3.09 | 3.24 | 3.12 | 0.08 |
| | S11 | 3.13 | 3.30 | 3.25 | 3.23 | 0.07 |
| | S12 | 3.45 | 3.17 | 2.97 | 3.20 | 0.20 |
| Subject 2 | S1 | 3.38 | 3.43 | 3.21 | 3.34 | 0.09 |
| | S2 | 3.92 | 4.02 | 3.68 | 3.87 | 0.14 |
| | S3 | 2.08 | 2.18 | 2.03 | 2.10 | 0.06 |
| | S4 | 2.84 | 2.64 | 2.83 | 2.77 | 0.09 |
| | S5 | 3.43 | 3.28 | 3.34 | 3.56 | 0.06 |
| | S6 | 3.56 | 3.36 | 3.76 | 3.14 | 0.16 |
| | S7 | 3.02 | 3.13 | 3.28 | 3.73 | 0.11 |
| | S8 | 4.02 | 3.54 | 3.64 | 3.12 | 0.21 |
| | S9 | 3.16 | 3.24 | 2.95 | 3.12 | 0.12 |
| | S10 | 3.73 | 3.63 | 4.10 | 3.82 | 0.20 |
| | S11 | 2.92 | 3.26 | 2.96 | 3.05 | 0.15 |
| | S12 | 3.01 | 2.76 | 2.65 | 2.81 | 0.15 |
| Subject 3 | S1 | 2.65 | 2.65 | 2.71 | 2.67 | 0.03 |
| | S2 | 2.67 | 2.78 | 2.92 | 2.79 | 0.10 |
| | S3 | 2.42 | 2.32 | 2.28 | 2.34 | 0.06 |
| | S4 | 3.17 | 3.53 | 3.15 | 3.28 | 0.17 |
| | S5 | 3.49 | 3.56 | 3.09 | 3.56 | 0.21 |
| | S6 | 3.54 | 3.47 | 3.68 | 3.18 | 0.09 |
| | S7 | 3.21 | 3.26 | 3.08 | 3.86 | 0.08 |
| | S8 | 3.75 | 3.84 | 3.98 | 3.07 | 0.09 |
| | S9 | 3.08 | 3.13 | 3.01 | 3.07 | 0.05 |
| | S10 | 3.37 | 3.47 | 3.43 | 3.42 | 0.04 |
| | S11 | 3.99 | 3.98 | 3.93 | 3.97 | 0.03 |
| | S12 | 4.45 | 4.21 | 4.40 | 4.35 | 0.10 |
| Subject 4 | S1 | 2.81 | 2.86 | 2.71 | 2.79 | 0.06 |
| | S2 | 2.56 | 2.67 | 2.76 | 2.66 | 0.08 |
| | S3 | 3.27 | 3.21 | 3.11 | 3.20 | 0.07 |
| | S4 | 3.79 | 3.52 | 3.47 | 3.59 | 0.14 |
| | S5 | 3.22 | 3.37 | 3.14 | 3.78 | 0.10 |
| | S6 | 3.81 | 3.97 | 3.57 | 3.30 | 0.16 |
| | S7 | 3.49 | 3.22 | 3.18 | 4.35 | 0.14 |
| | S8 | 4.47 | 4.12 | 4.47 | 3.58 | 0.16 |
| | S9 | 3.59 | 3.44 | 3.72 | 3.58 | 0.11 |
| | S10 | 3.46 | 3.34 | 3.55 | 3.45 | 0.09 |
| | S11 | 3.52 | 3.79 | 3.56 | 3.62 | 0.12 |
| | S12 | 3.36 | 3.61 | 3.59 | 3.52 | 0.11 |

## Supplementary Table 14

Comparison of the completion time of SHAP tasks with DexSoftNeuroHand and current neuroprosthetic hands.

| SHAP task | Existing prosthetic hand* (s) | Our previous work** (s) | Subject1 (s) | Subject2 (s) | Subject3 (s) | Subject4 (s) |
|---|---|---|---|---|---|---|
| S1: power light | 3.75 | 4 | 2.68 | 3.38 | 2.65 | 2.81 |
| S2: power heavy | 4.12 | 4.7 | 2.56 | 3.92 | 2.78 | 2.67 |
| S3: spherical light | 4.31 | 3.6 | 2.07 | 2.08 | 2.32 | 3.21 |
| S4: spherical heavy | 4.30 | 4.3 | 2.81 | 2.83 | 3.17 | 3.52 |
| S5: tip light | 4.63 | 4.6 | 3.48 | 3.34 | 3.49 | 3.22 |
| S6: tip heavy | 4.58 | 5.3 | 3.38 | 3.56 | 3.54 | 3.81 |
| S7: extension light | 4.75 | 5.3 | 2.75 | 3.13 | 3.21 | 3.22 |
| S8: extension heavy | 4.38 | 6.9 | 3.1 | 3.64 | 3.84 | 4.47 |
| S9: tripod light | 4.94 | 5.1 | 2.74 | 3.16 | 3.08 | 3.59 |
| S10: tripod heavy | 4.25 | Failed | 3.09 | 3.73 | 3.43 | 3.46 |
| S11: lateral light | 5.10 | Failed | 3.25 | 2.96 | 3.98 | 3.56 |
| S12: lateral heavy | 4.97 | Failed | 3.17 | 2.76 | 4.4 | 3.59 |

* Burgerhof, J. G. et al. The Southampton hand assessment procedure revisited: A transparent linear scoring system, applied to data of experienced prosthetic users. *J. Hand Ther.* 30, 49-57 (2017).

** Gu, G. et al. A soft neuroprosthetic hand providing simultaneous myoelectric control and tactile feedback. *Nat. Biomed. Eng.* 7, 589-598 (2023).

## Supplementary Table 15

Main objects involved in the application experiments of activities in daily living.

| Objects | Object Type | Weight (g) | Dimension (mm×mm×mm) | Texture material |
|---|---|---|---|---|
| Card | Flat | 4.1 | 48×60×2 | Plastic |
| Block | Convex | 8 | 25×25×25 | Wood |
| Water Can | Convex | 371.3 | 164×98×98 | Plastic |
| Tissue | Deformable | 1 | 174×130×0.2 | Paper |
| Pen | Convex | 13.9 | 145×15×15 | Plastic |
| Cucumber | Convex | 232 | 322×28×28 | Organic |
| Coffee pack | Deformable | 9.5 | 42×93×5 | Plastic |
| Thermal mug | Convex | 613 | 221×75×75 | Metal |
| Flower bunch | Deformable | 114 | 310×40×40 | Organic |
| Banana | Convex | 163 | 202×36×36 | Organic |
| Tofu | Deformable | 12 | 20×20×20 | Organic |
| Nail | Convex | 2.2 | 38×2.9×2.9 | Metal |
| Chinese chess pieces | Convex | 51 | 20×57×57 | Wood |
| Chess pieces | Non-convex | 46 | 75×30×30 | Wood |
| Pill bottle | Convex | 25 | 40×24×24 | Plastic |
| String | Deformable | 0.5 | 0.3×0.3×100 | Polyethylene |
| Bag with 2.5-kg weights | Deformable | 2503 | Not applicable | Plastic |
| Doll | Convex | 100 | 51×105×128 | Fabric |
| Sea snail | Non-convex | 20 | 16×18×32 | Organic |
| Baseball cap | Deformable | 83 | 202 × 180 × 120 | Cotton/Fabric |
| Headphone stand | Non-convex | 312 | 154 × 150 × 223 | Wood |
| Wireless mouse | Convex | 95 | 111 × 60 × 34 | Plastic |
| Phone stand | Non-convex | 52 | 110 × 72 × 21 | Plastic |
| Folded umbrella | Convex | 245 | 283 × 51 × 50 | Fabric/Metal |
| Game controller | Non-convex | 284 | 155 × 104 × 63 | Plastic |
| Data cable | Deformable | 150 | ~152 × 100 × 42 | Rubber/Plastic |
| Foam ball | Deformable | 21 | 61 × 60 × 61 | Foam |
| Over-ear headphone | Non-convex | 255 | 200 × 182 × 92 | Plastic/Leatherette |
| Green pepper | Convex | 124 | 151 × 50 × 51 | Organic |
| Tube (signagel) | Deformable | 280 | 204 × 81 × 40 | Plastic |
| Glass goblet | Non-convex | 180 | 81 × 80 × 171 | Glass |
| Stapler | Non-convex | 198 | 131 × 40 × 55 | Plastic/Metal |
| Pinecone | Non-convex | 40 | 82 × 61 × 60 | Wood/Organic |
| Phone case | Flat | 42 | 161 × 80 × 12 | Plastic/Silicone |
| Drink cup | Convex | 510 | 96 × 95 × 174 | Plastic |
| Clownfish toy | Deformable | 62 | 120 × 71 × 52 | Plastic |
| Rubber doll | Deformable | 50 | 81 × 73 × 80 | Rubber/Vinyl |
| Grapes | Deformable | 300 | 181 × 100 × 62 | Organic |
| Scalp massager | Non-convex | 78 | 91 × 90 × 80 | Plastic/Silicone |

**Types of Objects** *

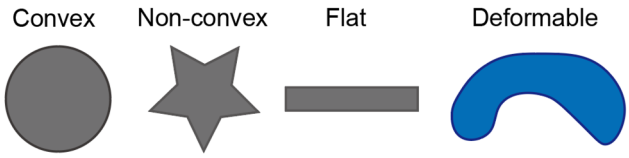


* Shintake, J. et al. Soft robotic grippers. *Adv. Mater.* 30, 1707035 (2018).

## Supplementary Table 16

Results from the System Usability Scale (SUS) questionnaires completed by four amputee subjects.

| | Strongly Disagree | Disagree | Neutral | Agree | Strongly Agree |
|---|---|---|---|---|---|
| Frequent use | | △ | ▲ | □ | ■ |
| Easy to use | | | △ | ▲ | ■□ |
| Well-integrated functions | | | | ■ | □▲△ |
| Quick learning | | | △ | ■▲ | □ |
| Confident use | | | △ | ■□▲ | |
| Unnecessarily complex | △ | ■▲ | □ | | |
| Need technical support | | ■△ | □ | ▲ | |
| System inconsistency | □ | ■▲ | △ | | |
| Cumbersome to use | | ■ | □▲ | △ | |
| Significant learning effort | ■ | □▲△ | | | |

■Subject 1 □Subject 2 ▲Subject 3 △Subject 4

## Supplementary Table 17

Results from the modified version of Quebec User Evaluation of Satisfaction with Assistive Technology (QUEST) questionnaires completed by four amputee subjects.

| | Not satisfied at all | Not very satisfied | More or less satisfied | Quite satisfied | Very satisfied |
|---|---|---|---|---|---|
| Dimensions | | | | ■▲△ | □ |
| Weight | | | | ■□▲ | △ |
| Adjustments | | | □△ | ■▲ | |
| Safety | | | | △ | ■□▲ |
| Durability | | ■ | □▲ | △ | |
| Simplicity of use | | | □ | ▲△ | ■ |
| Comfort | △ | ▲ | ■ | □ | |
| Effectiveness | | | ▲△ | □ | ■ |

■Subject 1 □Subject 2 ▲Subject 3 △Subject 4

## Supplementary Table 18

NASA Task Load Index (NASA-TLX) test results for different execution modes of the bulb installation task.

| | Low (0-30) | Low-med (31-50) | Medium (51-70) | High (71-85) | Very High (86-100) |
|---|---|---|---|---|---|
| Mental demand | - | - | ①③ | ② | - |
| Physical demand | - | ① | - | ③② | - |
| Temporal demand | - | ③ | ①② | - | - |
| Performance | - | ② | ③ | ① | - |
| Effort | - | - | ①③ | ② | - |
| Frustration | - | ①③ | ② | - | - |

① DexSoftNeuroHand manipulation mode

② DexSoftNeuroHand grasp-only mode

③ Rigid neuroprosthesis

**Supplementary Video 1**
Mechanical design and dexterity demonstration of DexSoftNeuroHand.

**Supplementary Video 2**
Demonstration of mechanical capabilities for dexterous manipulation.

**Supplementary Video 3**
Demonstration of the sEMG acquisition and control algorithm performed by the amputee subject.

**Supplementary Video 4**
Demonstration of continuous grasp and manipulation gestures by an amputee subject.

**Supplementary Video 5**
Demonstration of a subject tuning the amplitude and strength of a specific grasp for objects with different dimensions and weights.

**Supplementary Video 6**
Experimental process of the Box and Blocks Test.

**Supplementary Video 7**
Experimental process of the Southampton Hand Assessment Procedure.

**Supplementary Video 8**
Demonstration of versatile essential life skills.

**Supplementary Video 9**
Demonstration of pinching slender rods with different diameters.

**Supplementary Video 10**
Demonstration of continuous grasping of 20 different objects.

**Supplementary Video 11**
Demonstration of bimanual coordination tasks.

**Supplementary Video 12**
Demonstration of a female subject creating a hairstyle for her daughter.

**Supplementary Video 13**
Demonstration of consecutive scissor cuts.

**Supplementary Video 14**
Demonstration of two-object picking.

**Supplementary Video 15**
Demonstration of bulb installation.

**Supplementary Video 16**
Demonstration of amputee body movement during bulb installation tasks.